IEEE Access
Multidisciplinary | Rapid Review | Open Access Journal

Received 25 June 2022, accepted 11 July 2022, date of publication 25 July 2022, date of current version 8 August 2022.

Digital Object Identifier 10.1109/ACCESS.2022.3193671

RESEARCH ARTICLE

Generative Modeling of Pedestrian Behavior: A Receding Horizon Optimization-Based Trajectory Planning Approach

SAUMYA GUPTA[1], (Student Member, IEEE), MOHAMED H. ZAKI[1], (Member, IEEE), AND ADAN VELA[2]

[1]Department of Civil, Environmental, and Construction Engineering, University of Central Florida, Orlando, FL 32816, USA
[2]Department of Industrial Engineering & Management Systems, University of Central Florida, Orlando, FL 32816, USA

Corresponding author: Mohamed H. Zaki (mzaki@ucf.edu)

ABSTRACT Urbanization is bringing together various modes of transport, and with that, there are challenges to maintaining the safety of all road users, especially vulnerable road users (VRUs). There is a need for street designs that encourages cooperation between road users. Shared space is a street design approach that softens the demarcation of vehicles and pedestrian traffic by reducing traffic rules, traffic signals, road marking, and regulations. Understanding the interactions and trajectory formations of various VRUs will facilitate the design of safer shared spaces. In line with this goal, this paper aims to develop a methodology for generating VRUs trajectories that accounts for behaviors and social interactions. We develop a receding horizon optimization-based pedestrian trajectory planning algorithm capable of modeling pedestrian trajectories in a variety of shared space scenarios. Focusing on three scenarios-group interactions, unidirectional interaction, and fixed obstacle interaction-case studies are performed to demonstrate the strengths of the resulting generative model. Additionally, generated trajectories are validated using two benchmark datasets – DUT and TrajNet++. The three case studies are shown to yield low or near-zero Mean Euclidean Distance and Final Displacement Error values supporting the performance validity of the models. We also analyze gait parameters (step length and step frequency) to further demonstrate the model's capability at generating realistic pedestrian trajectories.

INDEX TERMS Optimization, mixed integer linear programming, shared space, social interaction rules, trajectory-planning, vulnerable road users, urban design and planning.

I. INTRODUCTION

The last few decades have witnessed an unprecedented growth of cities; one recent report [1] indicates that by 2050 70% of the world's population will be living in metropolitan regions. Questions regarding sustainability and evolving community demands have prompted the need for transportation policy and urban planning to transition from a narrow automobile-centric perspective to one that recognizes and accounts for alternative forms of active mobility [2]. Vulnerable road users (VRUs), namely (but not limited to) pedestrians and cyclists, are active traffic agents who are unprotected by an outside shield [3]. In the August 2021 research note [4] the National Highway Traffic Safety Administration indicated an increasing trend in VRU fatalities, both in absolute number and proportion, since 2000. Meanwhile, on a per-capita basis and per-vehicle-mile traveled, motor-vehicle deaths have decreased by almost 25% and 30% between 2000 and 2019 [5].

As the increasing trend in VRU fatalities is concerning, urban planners are also motivated to redesign roadways and traffic infrastructure to provide more equitable access to users, which has led to the introduction of *shared spaces* or 'woonerf'-a Dutch term meaning living streets. As depicted in Figure 1, shared spaces provide for VRUs and cars to make use of a common physical space without the conventional

The associate editor coordinating the review of this manuscript and approving it for publication was Shajulin Benedict.

safety systems of traffic lights, curbs, stop signs, and traffic rules [6]. When operating in shared spaces all road-users must remain alert, attentive, communicative, and responsive to each other. Such urban street design concepts aim to promote active mobility, alleviate congestion, and optimize the efficient utilization of intelligent transportation systems [7]. However, with the transformation of city streets into shared spaces, it becomes essential to identify the traffic safety challenges in shared spaces.

Among all VRUs and active mobility options, pedestrian s are the most common and vulnerable. In fact, recent reports state there has been an increase of 53% in pedestrian fatalities during the last ten years [8], [9]. Hence, it becomes imperative to study pedestrian mobility in shared space and identify the safety challenges, which primarily depends on the understanding of pedestrian behavior when interacting with and amongst mixed traffic.

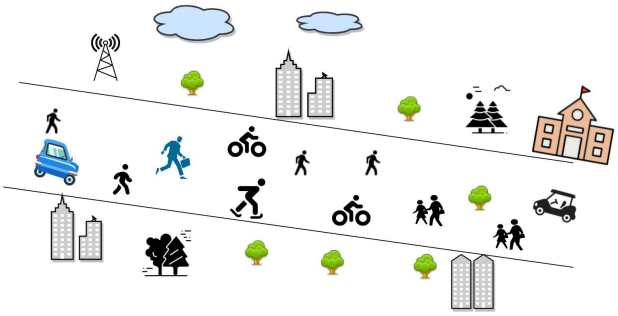

FIGURE 1. A Shared space concept-Woonerf-where the distinction between various modes of transportation is blurred. There is absence of sidewalks, curbs, lanes. Woonerf is a living street with improved safety for VRUs.

Pedestrian trajectories are the result of a closed-loop decision-making process that accounts for several factors such as physical, mental, psychological, and static and dynamic environmental conditions. Since the last two decades of twentieth century, significant effort has been placed into understanding and modeling pedestrian behaviors [10], [11], movements [12], and trajectories [13]. For an extensive survey focusing on pedestrian motion analysis one can refer to [14]–[17]. Effective modeling of pedestrian behaviors and their motions requires large observational data to capture minute intricacies. Recent advances in sensing and communication have led to an increased availability of pedestrian motion data which is assisting in the understanding pedestrian behaviors [18].

One common approach for studying pedestrian traffic is through simulation. There are sustained efforts by researchers and traffic agencies to develop realistic and practical pedestrian simulation models [19]–[24]. Developing pedestrian simulation models span many approaches, with noteworthy efforts making use of agent-based modeling techniques [25] and cellular automaton-based techniques [26], [27]. The availability of reliable datasets [28] has also enabled machine learning algorithms to learn and predict pedestrian trajectories [29].

A realistic pedestrian generative and simulation model requires consideration of human behavior and interaction rules. However, a careful investigation of the above mentioned literature reveals that there are two *critical gaps* in the existing pedestrian trajectory modeling and simulation approaches that limit their application to the previously discussed needs. First, current approaches do not effectively consider scenario specific pedestrian walking behavior, the nature of interactions, group interactions, and route optimization. Secondly, there is a lack of a well-defined yet flexible parameterized model that requires minimal training data while remaining transferable amongst broad classes of environments and scenarios.

In this paper, we report on the development of a generative pedestrian trajectory planning model within an optimization framework that considers human walking behaviors. The resulting approach uses mixed-integer linear programming (MILP) coupled with receding horizon control (RHC) for trajectory generation while computing dynamically feasible state and control actions. The proposed generative pedestrian trajectory model is a white-box model, whereby the cost function and constraints for a given scenario are not only observable, but can also be easily modified to reflect different scenarios of pedestrian movements and interactions. Moreover, the resulting model is designed to incorporate realistic pedestrian interaction traits by considering how pedestrians (agents) interact within a group and with their surrounding environment-e.g., during the group movement and interaction with a fixed obstacle. When evaluated against the Dalian University of Technology (DUT) and TrajNet++ benchmark datasets, we demonstrate that generated trajectories maintain near-zero Mean Euclidean Distance and Final Displacement Error with actual trajectories, thereby supporting and indicating validity of the model.

A. CONTRIBUTIONS

Trajectory control and modeling based on MILP optimization provides fast computational speed, which explains its successful application in robotics motion planning. To the best knowledge of authors, this is the first research effort to utilize mixed-integer linear programming embedded within RHC optimization for pedestrian-centric modeling. Through our research we are bringing together the domain of operations research, urban transportation, and pedestrian behavioral studies. The corresponding contributions are as follows:

- The proposed methodology successfully predicts time-efficient, dynamically-feasible, and realistic pedestrian group trajectories for given scenarios.
- When considering pedestrian trajectories within obstacle-free environments, the problem formulation is convex, and hence, global optimality of solutions is guaranteed.
- The methodology involves few parameters (all of which are adjustable according to need) that can be estimated

even with limited data availability or drawn from distributions to create randomly generated scenarios.
- The proposed methodology is robust and generic-meaning that the parameters estimated for one location serve well for others as well.
- A variety of group walking behavioral traits and collision avoidance scenarios are considered.
- The proposed receding horizon optimization-based trajectory planning approach can adapt to the uncertainties in the environment as the model plans the trajectory and the interactions among agents at the current time as well over a next few time-steps (i.e. over the planning horizon).

B. APPLICATION

The pedestrian trajectory planning model serves as a strong simulation model due to its white-box design while maintaining validity. Given the formulation and ability of the model, it is expected to be utilized by urban planners to test and evaluate various traffic scenarios and designs related to shared spaces with the goal of enabling efficient transportation management supporting active mobility.

The remainder of this paper is divided into six sections. Section 2 presents a literature review of the existing research in pedestrian modeling and highlights key research gaps. Section 3 includes the basic introduction to the mathematical concepts of convex-optimization, MILP, and RHC. Also, the problem formulation details and proposed methodology are explained in Section 3. Section 4 discusses implementation details. Section 5 covers the model calibration and model validation by performing three case studies using the dataset collected at a university campus [30]. Section 6 presents the case studies and the model's cross-validation on TrajNet++ [31]. Finally, the work's significance, impact, and key findings, along with future work are summarized in Section 7.

II. LITERATURE REVIEW

There are several important aspects of pedestrian mobility to consider when designing a modeling approach, they include: individual walking behaviors, group behaviors, crowd interactions, interaction with other traffic agents (e.g. cyclists and scooters), and interaction with the environment. Overall, understanding and modeling pedestrian motion requires consideration of both the macro and micro-movement characteristics [32], [33].

A. EVOLUTION OF PEDESTRIAN MODELS

Many pedestrian trajectory simulation models rely on the physics-based and the cellular automata-based modeling approaches [34]. Physics-based modeling approaches treat pedestrians as particles, and their interactions with other elements are estimated by considering different exerted physical forces. The updates to pedestrian trajectories depend on the direction and magnitude of the resulting force. The Social Force Model, developed by Helbing and Molnar in 1995 [35] was the first physics-based modeling approach considered to design a pedestrian mobility model. The social forces-attractive and repulsive forces-reflected the pedestrian interaction with the environment.

The cellular automata method employs a discrete spatial representation of the environment, whereby the environment is divided into cells of fixed size that can only be occupied by one pedestrian at a time. The pedestrian moves from one cell to another depending on pre-defined transitional rules (primarily dependent on a probability of choosing the target cell). The cellular automata modeling approach was applied by Blue and Adler [36] to build pedestrian simulation models for unidirectional flow, bidirectional flow, and extended the work to four-directional pedestrian flows [13], [37].

Other modeling approaches utilize concepts such as fuzzy logic, gas-kinetic model, control methods, and utility maximization (Hoogendoorn and Bovy's Nomas Model) [38]. The corresponding simulation models provided an excellent platform for performing evacuation studies and understanding large-scale crowd behavior; however, applications requiring a detailed understanding of pedestrian behavior and precise outputs cannot be tested. These limitations were originally associated with the limited availability of pedestrian datasets. At the start of the twenty-first century computer vision, along with pattern recognition techniques, has helped to create databases [28], [39] which support understanding and characterizing human interaction behavior [18], [40], [41]. That said, simulation or recreation of realistic pedestrian walking behavior is not a trivial task, as pedestrian walking behavior depends on the context, spatial configuration, obstacle avoidance, and group interactions [42], [43].

Application of agent-based modeling (ABM) techniques have been used to develop pedestrian trajectory simulations [25], [44]. Agent-based modeling supports simulation models capable of including pedestrian walking behavior rules while interacting with the environment, thereby resulting in better realizations [45]. One of the first attempts to apply ABM techniques was the STREETS model [46]. The STREETS model demonstrated that every agent could be represented as having unique behavioral characteristics, like speed, direction, and visual range, allowing for realistic simulations. The research by Helbing in 2012 [25] highlighted the ability of agent-based modeling in handling heterogeneous pedestrian systems, specifically when analyzing different agent types and different pedestrian behaviors, and when performing both microscopic and macroscopic studies of various traffic scenarios. However, in ABM, each agent takes the instantaneous information of the traffic social forces, and respond to that at that instant. There is no planning for the next few time-steps involved in ABM approaches.

Other studies have performed detailed pedestrian behavioral studies [47], [48] and estimated pedestrian gait parameters [49]. These studies have considered case scenarios at signalized and non-signalized crosswalks, and at railway stations, along with behavioral changes with group size, age, and gender. Defining the environment and its key

contextual factors are required to effectively study and analyze scenarios of interest. An agent's inherent characteristics and behaviors towards the considered environment has to be carefully embedded in any model to achieve the model objectives [50], [51].

B. HUMAN TRAJECTORY PREDICTION

Predicting the future positions of pedestrians, along with trajectory planning, has become increasingly important to studies related to autonomous vehicles, robotics, and advanced surveillance systems. The papers [29] and [52] provides a detailed survey of research works based on human motion planning and prediction. Examples include trajectory forecasting frameworks that predict trajectories based on observed partial trajectories or from observed agents' states such as position, velocity [53], [54]. There are also recent works based on deep learning-based algorithms [55], [56] for pedestrian trajectory prediction, this includes [31] which presents a detailed analysis of existing deep learning-based human trajectory forecasting models. The aforementioned paper also proposes two new models that effectively consider social interactions and forecast trajectories.

C. RESEARCH GAPS

The Social Force Model and cellular automata modeling has been successfully applied to existing pedestrian simulation models, many of which are still being used today in their design and decision-making process. However, a key shortcoming of many existing models is that they lack sufficient consideration of pedestrian interactions, and therefore they are not capable of capturing critical and commonplace behaviors, especially in shared spaces. On the other hand, ABM approaches incorporate behavior and interaction rules. However, ABM is often times overly complicated as it involves numerous parameters that make them difficult to extend to diverse agent-types and environments without significant hand-tuning. Alternatively, models require a considerable amount of data for training and parameter estimation, making machine learning-based algorithms highly data-dependent.

In summary, current approaches often have one or many of the following limitations:

- Location specific and /or requires extensive calibration for proper transferability.
- Make use of non-parametric (machine learning) approaches that are black boxes in nature, relying on large dataset. Meanwhile, parametric approaches (such as ABM) often require large number of parameters, often resulting in a complex, unintuitive model.
- ABM approaches lack the planning, i.e, how agents plan for the trajectory for the next few time steps in the presence of various social interactions.
- Learning-based models require a vast amount of data for training or parameter estimation purposes. This can be challenging when collected pedestrian data for training is limited.

III. PROBLEM FORMULATION

In this section, the adopted receding horizon control based (RHC) modeling framework is explained. The pedestrian trajectory planning and trajectory execution is developed at the foundation of RHC that incorporate pedestrian behavioral rules and environment interaction rules. Next, the MILP trajectory optimization embedded within a receding horizon control loop is explained which serves as the primary component by which pedestrian decision-making is modeled, the detailed formulation of decision variables, constraints, and private and common objective function is given.

A. MODELING FRAMEWORK

Our simulation framework begins by considering the generalized problem of multiple agents or pedestrians in the set $\mathscr{P}$, traversing an environment with a set of obstacles $\mathscr{O}$. When moving about the environment, the pedestrians are further sub-divided into groups of pedestrians or individual pedestrians. That is to say, some of the pedestrians are walking alone, while others might be walking together in groups. Consistent with existing research on pedestrian behaviors, when walking together, a group of pedestrians will naturally self-organize into a moving cluster in which each person maintains a relative separation between themselves and others in their group. As depicted in Figure 2a, such a self-organized group of pedestrians can be mathematically modeled as a moving graph structure $\mathscr{G} = (\mathscr{V}, \mathscr{E})$ where each node v_i in the vertex set $\mathscr{V}$ corresponds to the i^{th} pedestrian in the pedestrian set $\mathscr{P}$. Meanwhile, the edge set $\mathscr{E}$ contains linkages (i, j) between any two pedestrians i and j walking in the same group that seeks to maintain fixed proximity with each other. Accordingly, associated with each group of pedestrians are desired separations, $d_{i,j}^{des} = (d_{i,j}^{\parallel des}, d_{i,j}^{\perp des}) \in \mathbb{R}^2$, consisting the lateral and longitudinal separation, between any two pedestrians i and j, along the group's direction of travel. A pictorial representation of the induced graph structure and desired separation distance between agents is illustrated in Figure 2.

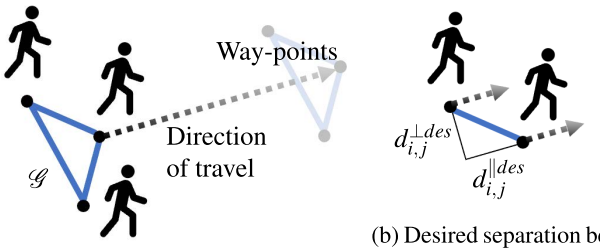

(a) Pedestrians walking in a group.

(b) Desired separation between pedestrians.

FIGURE 2. Pedestrian groups walk towards a common way-point while maintaining a desired separation from each other.

Within this framework, each pedestrian is associated with a final destination. However, by means of reaching their destination, the pedestrian will move through a series of segments defined by an ordered set of way-points. For the case of pedestrian i, the next desired way-point is given by w_i.

When located at position $x_{i,t}$ in a global coordinate frame at time-step t, the direction of travel for the pedestrian is given by the angle $\theta_i = \angle(w_i - x_{i,t})$. When walking together in a group, it is assumed that all pedestrians maintain the same way-point goal. However, the goal is sufficiently far away so that small angle approximations are permissible when modeling the pedestrian dynamics. That is to say, $\|\theta_i - \theta_j\| \leq \epsilon$, where ϵ is small, for all pedestrians i and j walking in the same group.

Consider the lower half of Figure 3 that considers a group of pedestrians in the set $\mathscr{P}$, traversing an environment, with a set of obstacles $\mathscr{O}$, where each static obstacle o is located at the position coordinates $(p^{Obs}_{o,x}, p^{Obs}_{o,y})$ so that $p^{Obs}_{o} \in \mathbb{R}^2 \; \forall \; o \in \mathscr{O}$. When walking from one way-point to the next, we assume pedestrians will become aware of changes in their environment (e.g., the appearance of obstacles) or adjust their path according to others in their walking group. In this context, we focus our attention on the tasks of trajectory planning and trajectory execution as each pedestrian moves between way-points; that is to say, the broader path planning problem of how pedestrians select way-points to arrive at their final destination is not addressed. Nonetheless, the modeling analogue of such a dynamic trajectory planning and execution process can be represented using a receding horizon control framework.

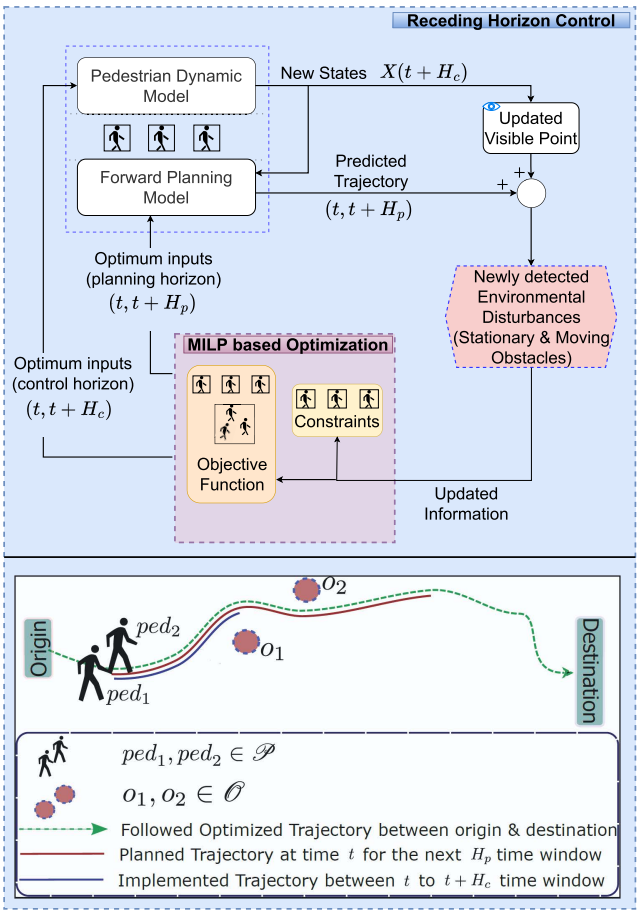

FIGURE 3. Modeling of the trajectory planning and trajectory execution process using a receding horizon control framework.

The receding horizon control framework, as depicted in Figure 3 begins with each pedestrian maintaining an awareness of their next desired way-point, the local environment (i.e., the obstacles), and the other pedestrians they are walking with, if any. Based on these factors, the pedestrian will be modeled to generate a path looking H_p seconds into the future, thereby establishing a planning-horizon. The pedestrian will begin to implement their planned path for a fixed control-horizon of H_c seconds, where $H_c \ll H_p$. After H_c seconds, the process of planning ahead for H_p seconds is repeated, followed by executing the resulting plan. This planning and execution process occurs ad infinitum until the pedestrian has cleared the environment; again, at each iteration, the pedestrian updates their estimate of the environment and the location of other pedestrians in their group. As the pedestrian reaches their desired way-point a new way-point is set, and the process begins again. A summary of the relevant parameters describing the receding horizon control framework for modeling pedestrian motion is provided in Table 1.

TABLE 1. Relevant parameters describing the pedestrian simulation model.

Symbol	Meaning
$\mathscr{P}$	Set of pedestrians
$\mathscr{O}$	Set of obstacles
$\mathscr{F}_o$	Set of facets associated with obstacle o.
$\mathscr{G} = (\mathscr{V}, \mathscr{E})$	Graph structure defining pedestrian groups.
H_p	Planning horizon [seconds]
H_c	Control horizon [seconds]
$x_{i,t} \in \mathbb{R}^2$	X-Y position of the i^{th} pedestrian at time-step t.
$w_i \in \mathbb{R}^2$	Next way-point of the i^{th} pedestrian.
$\theta_i = \angle(w_i - x_{i,t})$	Direction of travel of i^{th} pedestrian at time-step t.
$d^{des}_{i,j} = (d^{\parallel des}_{i,j}, d^{\perp des}_{i,j}) \in \mathbb{R}^2$	The desired longitudinal and lateral separation between pedestrians i and j along their common direction of travel.

Within this paper, the goal is to develop and describe the trajectory planning and trajectory execution processes at the foundation of the receding horizon control framework used to model pedestrians. And more specifically, to provide a flexible representation that can be easily adapted to consider other types of active mobility agents. Here, the planning proces is modeled and solved using Mixed-Integer Linear Programming (MILP). As part of the trajectory planning process, the underlying MILP optimization model assumes that each pedestrian maintains an accurate representation of the world (i.e., knows the location of obstacles and their group members); this information is encoded through constraint equations that model pedestrian dynamics and obstacle constraints. As pedestrians walk within a group, we assume they maintain private and common objectives. In this case, private objectives can include or consider: walking speeds, distance to obstacles, and time-to-arrival or distance-from-destination.

Common objectives are associated with maintaining the moving graph structure discussed above, which is accomplished by maintaining the desired separation distance between other pedestrians in their group.

B. TRAJECTORY OPTIMIZATION

Within the receding horizon control framework introduced in Section III-A is the MILP optimization, which serves as the primary component by which pedestrian decision-making is modeled. The MILP optimization seeks to represent the private and common objectives and the dynamic and static constraints associated with pedestrians as they move within their environment. By clearly defining the objective functions (and associated coefficients) along with any constraints, the formulation, when solved, provides an optimal trajectory representative of the goals and objectives of each individual pedestrian. In this sub-section, details of the optimization formulation is provided, beginning with introducing important decision variables, followed by detailing of the constraint equations, and finally, describing the private and common objective functions for the pedestrians.

1) DECISION VARIABLES

For a given instantiation of the trajectory planning and execution cycle, each pedestrian i in the pedestrian set $\mathscr{P}$ is first described according to their current x-y position $x_{i,t_0} \in \mathbb{R}^2$ at time-step t_0 and their desired next way-point, $w_i \in \mathbb{R}^2$. When optimizing the trajectories for H_p seconds over the planning horizon it is necessary to introduce new decision variables representing the planned position and velocity of each pedestrian. To distinguish between the actual position of the pedestrians, $x_{i,t}$, and the planned position of the pedestrians is denoted, $z_{i,k} \forall k \in \{1, \ldots, H_p\}$, representing the position of pedestrian i over H_p seconds when using 1-second increments. We also introduce the decision variables related to the position, velocity, and acceleration of each pedestrian relative to their direction of travel; for clarity, all decision variables described according to the coordinate frame in the direction of travel are indicted by the harpoon accent (e.g. $\vec{z}_{i,k}$). Accordingly, the decision variables for the position, velocity, and acceleration of pedestrian i in the rotated coordinate frame along the direction of travel are given by $\vec{z}_{i,k} = (\vec{z}^{\parallel}_{i,k}, \vec{z}^{\perp}_{i,k})$, $\vec{v}_{i,k} = (\vec{v}^{\parallel}_{i,k}, \vec{v}^{\perp}_{i,k})$ and $\vec{u}_{i,k} = (\vec{u}^{\parallel}_{i,k}, \vec{u}^{\perp}_{i,k})$, all defined over $\mathbb{R}^2 \; \forall k \in \{0, \ldots, H_p - 1\}$; each term inside the vectors corresponds to the longitudinal and lateral values along the nominal direction of travel.

The distinction between the position of pedestrians in a global coordinate frame versus a local coordination frame assists in establishing constraints and objective costs related to the position of pedestrians relative to obstacles and other pedestrians in their group. When constructing optimization constraints associated with obstacle avoidance, it is easiest to describe these obstacle constraints using a common global coordinate frame. Meanwhile, because the desired separation between pedestrians walking in a group is described in a relative frame, using a coordinate system aligned with this relative coordinate frame is preferred. Similarly, velocity and acceleration constraints for each pedestrian are easily described in the local coordinate frame. Translation of the pedestrian position at any time-step between the global and a rotated local coordinate frame is possible using the linear transformation

$$z_{i,k} = R(-\theta_i)\vec{z}_{i,k} \quad \forall\, k \in \{0, \ldots, H_p - 1\} \tag{1}$$

where $R(\theta_i)$ is the standard rotation matrix

$$R(\theta_i) = \begin{bmatrix} \cos\theta_i & -\sin\theta_i \\ \sin\theta_i & cos\theta_i \end{bmatrix}$$

parameterized by the direction of travel θ_i.

Based on the descriptions above a complete list of decision-variables is provided in Table 2.

TABLE 2. Relevant decision variables for the pedestrian trajectory planning optimization model.

Symbol	Meaning
$z_{i,k} \in \mathbb{R}^2$	Planned position of pedestrian i at time-step k in global X-Y coordinate frame
$\vec{x}_{i,k} = (\vec{x}^{\parallel}_{i,k}, \vec{x}^{\perp}_{i,k}) \in \mathbb{R}^2$	Planned position of pedestrian i at time-step k in rotated coordinate frame in direction of travel
$\vec{v}_{i,k} = (\vec{v}^{\parallel}_{i,k}, \vec{v}^{\perp}_{i,k}) \in \mathbb{R}^2$	Planned velocity of pedestrian i at time-step k in rotated coordinate frame in direction of travel
$\vec{u}_{i,k} = (\vec{u}^{\parallel}_{i,k}, \vec{u}^{\perp}_{i,k}) \in \mathbb{R}^2$	Planned acceleration of pedestrian i at time-step k in rotated coordinate frame in direction of travel
$b_{o,f,i,k} \in \{0,1\}$	Binary variable used to indicated that pedestrian i is outside of the boundary of obstacle o, in reference to facet f of the obstacle, at time-step k

2) DYNAMIC CONSTRAINT EQUATIONS

A portion of the constraint equations seek to represent the dynamic constraints describing pedestrian motion. For the i^{th} pedestrian the second-order discrete-time update equation for their position relative to their direction of travel is given by the set of constraints

$$\begin{aligned} \vec{z}_{i,k+1} &= \vec{z}_{i,k} + \vec{v}_{i,k}\Delta T + 1/2\vec{u}_{i,k}\Delta T^2 \\ \vec{v}_{i,k+1} &= \vec{v}_{i,k} + \vec{u}_{i,k}\Delta T \\ &\quad and \quad k \in \{0, \ldots, H_p - 1\} \end{aligned} \tag{2}$$

The discrete-time update equation in Equation (2) assumes a regularly updating process that occurs at a regular time-step of ΔT seconds (e.g. 1 sec, 5 sec), during which in between time-stamps, the acceleration is asserted to be constant.

The motion of each pedestrian can also be constrained according to their minimum and maximum walking velocity, denoted by $\underline{v}_i, \bar{v}_i$, and their minimum and maximum acceleration. Applying the small angle approximation, whereby it is assumed that the lateral velocity of pedestrians is small compared to their longitudinal velocity, it is sufficient to write

$$\underline{v}_i \leq \vec{v}^{\parallel}_{i,k} \leq \bar{v}_i \quad \forall i \in \mathscr{P}. \tag{3}$$

In many cases, pedestrians can be restricted to only walk forward so that $\underline{v}_i > 0$. In the case when the small angle approximation is likely to be violated, it is possible to replace the velocity constraint in Equation (3) with

$$\left\| \vec{v}_{i,k} \right\|_2^2 \leq \bar{v}_i \quad \forall i \in \mathscr{P}. \tag{4}$$

which corresponds to a convex quadratic constraint that can be represented in CPLEX, CVX, or other commonly used optimization solvers. The limitation of the constraint in Equation (4) is that non-zero minimum bounds on the magnitude of the velocity (e.g. $\underline{v}_i \leq \left\| v_{i,k} \right\|_2^2 \leq \bar{v}_i$) cannot be enforced without converting the constraint to be non-convex – thereby making it unsolvable in CVX without significant approximations, or expansion and manipulation of the constraint. That said, Equation (4) can be approximated using the ℓ_∞ or ℓ_0 norms, or can be approximated with a convex polygon.

Similar constraints on the acceleration rate of pedestrians is also possible using similar representations. That is to say, it is possible to include the acceleration constraint

$$\left\| \vec{u}_{i,k} \right\|_2^2 \leq \bar{u}_i \quad \forall i \in \mathscr{P}. \tag{5}$$

3) OBSTACLE CONSTRAINT EQUATIONS

The potential presence of obstacles within the environment requires pedestrians to plan their trajectories accordingly. In contrast to the pedestrian constraints and cost equations, the obstacle avoidance constraints are inherently non-convex. Essentially, obstacle avoidance generates binary variables and a set of constraints that correspond to moving *left* or *right* around any obstacle relative to any given side or facet of the obstacle. For a convex obstacle o that can be approximated by a polygon with a set of facets, $\mathscr{F}_o = \{1, \ldots, F_o\}$, it is possible to define a set of linear constraints

$$h_{o,f}^T y \leq g_{o,f} \quad \forall f \in \mathscr{F}_o \tag{6}$$

representing half-spaces that can be used to define the set of points $y \in \mathbb{R}^2$ that are blocked by the obstacle.

For obstacle avoidance, the planned position of a pedestrian at any point in time, $z_{i,k}$, must be outside of the convex polygon. In relation to a single facet $f \in \mathscr{F}_o$ of the polygon representing obstacle o, the i^{th} pedestrian is outside of the obstacle if their position at time-step k satisfies the constraint

$$g_{o,f} - h_{o,f}^T x_{i,k} \leq 0 \tag{7}$$

Accordingly, to avoid obstacle o, Equation (7) must hold true for at least one of the facets f to ensure that the pedestrian is located outside of the obstacle. The representation of such a constraint is written as

$$\begin{cases} g_{o,1} - h_{o,1}^T x_{i,k}, & \leq 0 \\ or & \\ \vdots & \\ or & \\ g_{o,f} - h_{o,f}^T x_{i,k}, & \leq 0 \\ or & \\ \vdots & \\ or & \\ g_{o,F} - h_{o,F}^T x_{i,k}, & \leq 0. \end{cases} \tag{8}$$

Implementation of the constraint in Equation (8) can be achieved using Big-M notation within a MILP solver after introducing binary variables $b_{o,f,i,k} \in \{0, 1\}\, \forall f \in \mathscr{F}$ and $k \in \{1, \ldots, H_p\}$; the binary logical condition $b_{o,f,i,k} = 1$ indicates that pedestrian i is avoiding obstacle o at time-step k relative to facet f. Within a MILP formulation, this is implemented for all pedestrians and all obstacles using the following constraint equations:

$$\begin{aligned} g_{o,f} - h_{o,f}^T x_{i,k} &\leq M(1 - b_{o,f,i,k}) \quad \forall f \in \mathscr{F}_o, o \in \mathscr{O} \\ &\quad i \in \mathscr{P}, \quad k \in \{1, \ldots, H_p\} \\ \sum_{f \in \mathscr{F}_o} b_{o,f,i,k} &\geq 1 \quad \forall o \in \mathscr{O}, i \in \mathscr{P} \\ &\quad k \in \{1, \ldots, H_p\} \end{aligned} \tag{9}$$

where M is sufficiently large such that the f^{th} constraint holds when $b_{o,f} = 0$ regardless of the position of the pedestrian. For practical purposes, the value of M can be set based on the dimensions of the environment. Alternatively, when implementing the constraints in Equation (8) in CVX, instead of using Big-M notation, it is suggested that readers make use of indicator constraints.

While not explicitly stated, a buffer distance can be added around each obstacle. If it is assumed that any extra buffer distance, $e_{o,i}$, depends on the specific obstacle o and pedestrian i then each obstacle constraint from Equation (7) is adjusted to

$$g_{o,f} - h_{o,f}^T x_{i,k} \leq - \left\| h_{o,f} \right\| e_{o,i}. \tag{10}$$

4) PRIVATE AND COMMON OBJECTIVE FUNCTIONS

Research suggests that pedestrians pursue personal objectives (e.g., minimization of their individual effort, reaching the desired destination) as well as global objectives shared with other agents (e.g., maintaining desired separations when walking in formation) [57]–[60]. Accordingly, we have formulated a generalizable objective function that takes into account all these factors.

Beginning with personal objectives, the objective function can account for the regulation of walking speeds, as well as running costs and the terminal cost of reaching

a desired way-point.

$$\sum_{k=1}^{H_p}\sum_{i\in\mathscr{P}}\Big(k_i^{acc}\left\|u_{i,k}-u_i^{des}\right\| + k_i^{speed}\left\|v_{i,k}-v_i^{des}\right\| + k_i^{run}\left\|x_{i,k}-w_i\right\|\Big) + \sum_{i\in\mathscr{P}} k_i^{term}\left\|x_{i,H_p}-w_i\right\| \tag{11}$$

In the private objective costs above, each norm can be adjusted according to desired modeling (i.e., ℓ_1, ℓ_2, or ℓ_∞). Additionally, each weighting can be adjusted to reflect the relative value.

When walking as part of a group, pedestrians can optimize their planned trajectories in order to maintain a desired formation. This is accomplished by penalizing any deviations between the actual and desired separation. This can be accomplished using the following objective equation:

$$\sum_{k=1}^{H_p}\sum_{(i,j)\in\mathscr{E}} k_{i,j}^{sep}\left\|\vec{z}_{i,k}-\vec{z}_{j,k}-d_{i,j}^{des}\right\| \tag{12}$$

The summation over the edge-set $\mathscr{E}$ in the graph structure $\mathscr{G}$ provides for significant flexibility. For example, it is not necessary to ensure consistency in the desired separation between pedestrians. So for any three pedestrians h, i, and j in the same pedestrian group there is no requirement that $d_{i,j}^{des}+d_{j,h}^{des}=d_{i,h}^{des}$. In fact, it is not even necessary that pedestrians in the same group seek to maintain a desired separation.

In specific cases (e.g. a parent and small child walking together), it may be more appropriate to represent separation distances within constraints instead of within objective costs. For the case in which two pedestrians must remain within a specified range $r_{i,j}$ of each other, the equivalent convex constraint is expressed as

$$\left\|\vec{z}_{i,k}-\vec{z}_{j,k}\right\|\le r_{i,j}\quad\forall\, k\in\{1,\ldots,H_p\} \tag{13}$$

5) MODEL SUMMARY

A summary of the complete formulation is provided below. Due to space constraints, a short-hand notation listed in Table 3 is used to indicate the ranges for which each the constraints hold. For example, all equations that hold true over $i\in\mathscr{P}, k\in\{1,\ldots,H_p\}$ are indicted by the $*$ symbol. As written below, all decision variables are assumed to be unrestricted, except for any binary variables. Furthermore, in summary below, we refrain from specifying which norm is used in the objective function and constraints. While in many cases, the ℓ_2 norm is appropriate, representations using the ℓ_1 or ℓ_∞ are permissible as well. Also, as noted in Section III-B2, ℓ_2 norms that restrict walking velocities and accelerations can be approximated through a series of linear convex constraints. The advantage of using an alternative to the ℓ_2 norm is that a broader array of optimization solvers can be used since the problem can be represented using a linear objective function and constraints.

TABLE 3. Short-hand markers indicating the ranges over which constraints apply.

Sets	Short-hand notation
$i\in\mathscr{P}, k\in\{1,\ldots,H_p\}$	$*$
$i\in\mathscr{P}, k\in\{0,\ldots,H_p-1\}$	$\bullet$
$i\in\mathscr{P}, k\in\{0,\ldots,H_p\}$	$\diamond$
$i\in\mathscr{P}, k\in\{1,\ldots,H_p\}, o\in\mathscr{O}, f\in\mathscr{F}_o$	$\triangle$
$i\in\mathscr{P}, k\in\{1,\ldots,H_p\}, o\in\mathscr{O}$	†

$$\begin{aligned}
\min\ & \sum_{k=1}^{H_p}\sum_{i\in\mathscr{P}}\Big(k_i^{acc}\left\|u_{i,k}-u_i^{des}\right\| + k_i^{speed}\left\|v_{i,k}-v_i^{des}\right\| + k_i^{pos}\left\|x_{i,k}-w_i\right\|\Big) + \sum_{i\in\mathscr{P}} k_i^{term}\left\|x_{i,H_p}-w_i\right\| \\
& \times \sum_{k=1}^{H_p}\sum_{(i,j)\in\mathscr{E}} k_{i,j}^{sep}\left\|\vec{z}_{i,k}-\vec{z}_{j,k}-d_{i,j}^{des}\right\| \\
s.t.\ & \vec{z}_{i,k+1}=\vec{z}_{i,k}+\vec{v}_{i,k}\Delta T+1/2\,\vec{u}_{i,k}\Delta T^2 && \bullet \\
& \vec{v}_{i,k+1}=\vec{v}_{i,k}+\vec{u}_{i,k}\Delta T && \bullet \\
& \left\|\vec{v}_{i,k}\right\|\le\bar{v}_i && * \\
& \left\|\vec{u}_{i,k}\right\|\le\bar{u}_i && * \\
& z_{i,k}=R(-\theta_i)\,\vec{z}_{i,k} && \diamond \\
& g_{o,f}-h_{o,f}^T x_{i,k}\le M(1-b_{o,f,i,k}) && \triangle \\
& \sum_{f\in\mathscr{F}_o} b_{o,f,i,k}\ge 1 && \dagger \\
& b_{o,f,i,k}\in\{0,1\} && \triangle
\end{aligned}$$

C. IMPLEMENTATION

Implementation of the receding-horizon control framework with the embedded MILP is completed in `MATLAB` using the `CVX` optimization library. While the `CVX` library is primarily targeted at solving convex optimization problems, it has recently gained support for both Mixed-Integer Linear Programs and Mixed-Integer Quadratic Programs. The proposed framework is applicable to a broad range of traffic scenarios. In our research, the three traffic scenarios manifesting a large portion of pedestrians' walking behavior and social interaction rules are identified. The traffic scenarios where a group of two agents walks together, a group of three agents walks together, and an agent avoids a stationery obstacle are considered. They are developed as three case studies, discussed in Sections IV and V. While experimenting with the case studies, we made a few adjustments-the terminal cost of reaching the desired waypoint is used while the running cost weight $k_i^{pos}=0$; the factor for speed regulation to have desired speed is made $k_i^{speed}=0$; the minimization of acceleration is included but the objective to maintain the desired acceleration is not implemented ($u_i^{des}=0$). Each

norm in the private objective cost is adjusted to the ℓ_1 norm. The common objective cost (Equation 12) is adjusted to ℓ_1 norm. The velocity and acceleration are constrained to an average minimum and maximum values, each in the lateral and longitudinal direction. They are adjusted as ℓ_∞ norm. The idea is to adjust the weights and the norm in the proposed generalized model as it results in a good Mixed-Integer Linear Programming problem.

Despite being the same here, within the receding-horizon control framework, the actual dynamics of the pedestrians are distinguished from the modeled dynamics contained in the trajectory planning optimization described in Section III-B, see Figure 3. Real-world differences emerge due to uncertainty in an environment (e.g., approximate location of obstacles) or perturbations in dynamics (e.g., a pedestrian tripping). Within a simulated environment, we assumed that the pedestrians' knowledge of the environment is perfect; that is to say, pedestrians are aware of the exact position and location of all obstacles and other pedestrians. The benefit of the proposed receding-horizon control modeling of uncertainties, and pedestrian response to the uncertainties can be modeled. Specifically, the capability of distinguishing between dynamics of pedestrians as different from the modeled dynamics of pedestrians contained in the trajectory planning optimization is particularly beneficial when modeling pedestrians with vision limitations, as well as pedestrians and active mobility users that become distracted or lose awareness of their environment.

IV. CALIBRATION AND VALIDATION

The next step to model development is calibrating the model parameters and validating the model outputs. This section will describe the model parameters, the dataset used, calibration process, performance metrics, and validation process of the developed pedestrian trajectory generating algorithm. The validation process compares the generated agent (i.e., pedestrian) trajectories with the ground truth for a traffic scenario. The proposed framework is generalizable to many pedestrian traffic scenarios. However, to show the validity of the proposed model, we have identified three case studies. Three case studies are performed-Case study 1 (Two agents walk together), Case study 2 (Three agents walk together), and Case study 3 (An agent avoids an obstacle).

A. KEY MODEL PARAMETERS

The key parameters of the developed pedestrian trajectory planning model are as follows:

- Total time-steps to run a simulation (T)
- The desired longitudinal separation between pedestrians i and j ($d_{i,j}^{\parallel des}$)
- The desired lateral separation between pedestrians i and j ($d_{i,j}^{\perp des}$)
- Control Horizon (H_c)
- Planning Horizon (H_p)
- Maximum and Minimum mean velocity
- Maximum and Minimum mean acceleration
- Buffer zone: The gap that the pedestrian tries to keep while passing the stationary obstacle

B. DATA DESCRIPTION

We considered data from the dataset of paper [30] which was collected at the campus of Dalian University of Technology (DUT) in China. The dataset is one of the crowd interaction benchmark datasets. The scenario includes an area of pedestrian crosswalks at an intersection. Figure 4 shows the data collection location and Figure 5 shows the sample of extracted trajectories. A *DJI Mavic Pro* Drone with a down-facing camera was used as the recording gear. The video resolution was 1920 × 1080 with an *fps* of 23.98. Pedestrians in the data are mainly college students. The trajectories were extracted from the recorded data using video stabilization, pedestrian tracking, coordinate transformation, and Kalman filtering techniques.

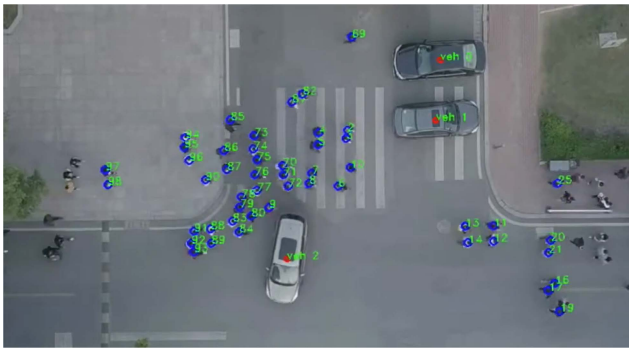

FIGURE 4. Data collection location.

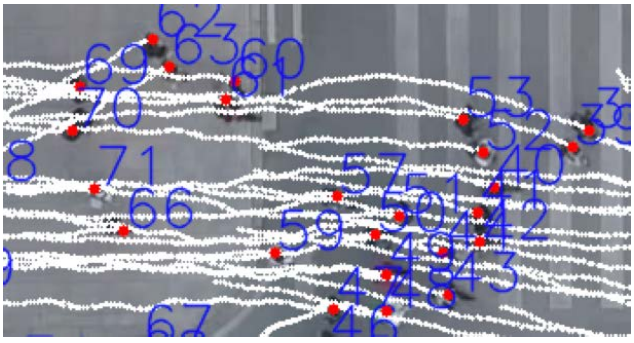

FIGURE 5. Sample extracted trajectories.

C. MODEL CALIBRATION

1) METHODOLOGY

Firstly, we identified traffic scenarios in the dataset where pedestrians are moving as a group of two, as a group of three, and as individual agents avoiding stationary obstacles. For each case study, maximum and minimum velocity, maximum and minimum acceleration, $d_{i,j}^{\perp des}$ and $d_{i,j}^{\parallel des}$ values are extracted, and the average values are calculated. Also, sampling time and pedestrian's initial and final destination values are determined from the dataset.

We have extracted forty samples for two agents group, thirty samples for three agents group, and twenty samples for individuals avoiding the obstacles. Considering the case study of two agents group, we divided the forty collected samples into thirty samples for training the model and ten samples for testing the developed model. We have used the normal distribution method to dynamically calibrate the $d_{i,j}^{\perp des}$ and $d_{i,j}^{\parallel des}$ values. The initial location values of the agent are updated at every control horizon time (H_c) based on receding horizon control.

2) CALIBRATED MODEL PARAMETERS

Table 4 shows the calibrated values of parameters for Case Study 1 (two agents walk together). We extracted the $d_{i,j}^{\perp des}$ and $d_{i,j}^{\parallel des}$ values and calculated the average values for all the samples for this case study. The values of $d_{i,j}^{\perp des}$ and $d_{i,j}^{\parallel des}$ aligned well with the normal distribution, further verified by the chi-square test($h = 0$). The chi-square goodness-of-fit test was done which returns the $h = 0$ value meaning the data comes from a normal distribution. In the Case Study 1, the planning horizon (H_p) was considered as 2 sec, and control horizon (H_c) was taken as 1 sec. Similarly parameters were computed for Case Study 2 and 3, shown in Tables 5 and 6 respectively.

TABLE 4. Model calibration for case study 1.

Parameters	Calibrated Values
$d_{i,j}^{\perp des}$	$\mu = 0.52, \sigma = 0.15$
$d_{i,j}^{\parallel des}$	$\mu = 0.097, \sigma = 0.046$
Average minimum velocity	0.97 m/sec
Average maximum velocity	1.70 m/sec
Average minimum acceleration	-0.3 m/sec^2
Average maximum acceleration	0.3 m/sec^2

TABLE 5. Model calibration for case study 2.

Parameters	Calibrated Values
$d_{i,j}^{\perp des}$ between agent 1 and agent 2	$\mu = 0.612, \sigma = 0.194$
$d_{i,j}^{\parallel des}$ between agent 1 and agent 2	$\mu = 0.294, \sigma = 0.237$
$d_{i,j}^{\perp des}$ between agent 2 and agent 3	$\mu = 0.241, \sigma = 0.178$
$d_{i,j}^{\parallel des}$ between agent 2 and agent 3	$\mu = 0.719, \sigma = 0.221$
Average minimum velocity	0.97 m/sec
Average maximum velocity	1.48 m/sec
Average minimum acceleration	-0.3 m/sec^2
Average maximum acceleration	0.3 m/sec^2

TABLE 6. Model calibration for case study 3.

Parameters	Calibrated Values
Average minimum velocity	0.82 m/sec
Average maximum velocity	1.75 m/sec
Average minimum acceleration	-0.3 m/sec^2
Average maximum acceleration	0.4 m/sec^2
Gap between the agent and obstacle	0.55 m

D. PERFORMANCE METRICS

To evaluate the results, we use the following performance metrics.

- MED: Mean Euclidean Distance is the average Euclidean distance between the model predicted coordinates and the actual coordinates of the pedestrian at every instant. Lower is better.
- FDE: Final Displacement Error is the Euclidean distance between the model predicted final destination and the actual final destination at the corresponding time instant.
- rmse_$d_{i,j}^{\perp}$: It is the root mean square error of the lateral distance between the two agents' actual and the generated trajectories.
- rmse_$d_{i,j}^{\parallel}$: It is the root mean square error of the longitudinal distance between the two agents' actual and the generated trajectories.
- Gait parameters: Analysis of basic gait parameters (step length, step frequency, and walking speed) helps understand a person's walking style. The step length and step frequency are affected by many attributes such as gender, age, group size, commonalities between agents [61], [62]. Step length is defined as the distance from the initial contact point of one foot to the initial contact point of the other foot. Step frequency is measured by the number of steps taken per minute. Following equation shows the relationship between the three determinant gait parameters [63], [64]:

  walking speed = step frequency x step length.

  To further validate our research work, we have compared the gait parameters estimated in the case studies with the ones mentioned in [49].

E. VALIDATION PROCESS

We have performed an extensive validation on a unidirectional pedestrian movement-group movement of two to three pedestrians, interaction with a stationary obstacle. The developed trajectory planning model is tested on the case studies obtained from the DUT crowd interaction dataset [30]. The case studies are where two agents walk together, three walk together, and an agent avoids a stationary obstacle. The generated trajectories are compared with the actual trajectories of agents for the particular traffic scenarios, and the proposed performance metrics will help to inspect the model performance. The details and results of three case studies are discussed in the following sections.

V. EXPERIMENTAL RESULTS

This section provides the experimental results form the chosen case studies. Note that the developed modeling framework is generalizable making it applicable across a broad range of pedestrian scenarios. To demonstrate this, we highlight three case studies that account for a large portion of pedestrian scenarios.

A. CASE STUDY 1: TWO AGENTS WALK TOGETHER

1) DESCRIPTION

We consider the scenario where two agents walk together. To perform the calibration and validation, we divided the

forty collected samples into thirty samples for training the model and ten samples for testing the developed model. The calibrated values are provided in the Table 4. The sample screenshots in Table 8 are from actual video data. In the sample screenshots, we can observe that the two agents are walking together, and they always maintain a certain separation between them. This behavior is expected from humans when they walk in a group.

2) RESULT

Once the model was calibrated, we performed the validation on the testing data. The trajectories are shown in Table 8. The first column shows the screenshots from the real dataset. The second column shows the corresponding model-generated trajectories. These are MATLAB-generated plots showing the generated trajectories and respective real trajectories of the same set of agents. In each graph, the marked lines are real trajectories, and non-marked lines are the corresponding model generated trajectories. For the given scenario's initial and final destination, the model generates the pedestrian trajectories by evaluating the environment and maintaining the human-human group behavior.

TABLE 7. Case study 1 performance metrics average values for DUT dataset.

Performance metrics	Average values
MED	0.28
FDE	0.45
rmse_$d_{i,j}^{\perp}$	0.36
rmse_$d_{i,j}^{\parallel}$	0.007

The plots in Table 8 show the accuracy of the generated trajectories. The lower values of performance metrics validate the good performance of the algorithm. Table 7 provides the average values of the performance metrics, MED and FDE. A zero value would indicate that the predicted and actual data are almost identical. However, the value of zero is almost not possible practically; therefore, the closer the average values are to zero, the better fit the data has achieved. The error metrics values are quite low, with MED = 0.28, FDE = 0.45, rmse_$d_{i,j}^{\perp}$ = 0.36, rmse_$d_{i,j}^{\parallel}$ = 0.007. Values confirm what we can visualize from the model generated results in Table 8. Table 10 illustrates the obtained gait parameters in case study 1. It can be noted that step length remains in the 0.6 to 0.7 meter range. On the other hand, pedestrians increase their step frequency to attain a higher speed to cross the pedestrian crossing in time. The obtained gait parameters are within the range as mentioned in [49]. The step length and step frequency define the walking speed as described in section IV-D. Those parameters also characterize the person walking style, which changes depending on the scenario, age, gender, and level of group commonalities. For example, the instantaneous value of a gait parameter is influenced by activities such as the walking behavior in a group and obstacle avoidance.

Table 9 summarizes the results for the testing dataset. The table shows the average values of root mean square error between the ground truth and the generated trajectory for x-position, y-position, longitudinal velocity of each agent at every instant. The values are near-zero, validating the high accuracy of the proposed model.

B. CASE STUDY 2: THREE AGENTS WALK TOGETHER

1) DESCRIPTION

We study the case scenarios where three pedestrian walks in a group, the left column in Table 12 shows some sample screenshots from real video data. The model is calibrated, and parameters values are listed in Table 5. The sample figures are from the actual data. To perform the calibration and validation of the case study of three agents' group behavior, we divided the thirty collected samples into twenty-three samples for training the model and seven samples for testing the developed model.

2) RESULT

Once the model was calibrated, we performed the validation on the testing data. The results are shown in Table 12. The results show the graphs which compare the actual and predicted trajectories. The left column in the table shows the sample scene from the video dataset, and the right column shows the model generated trajectories and their comparison with the actual trajectories. The plots demonstrate the model's accuracy and illustrate the group formation, as explained in Figure 2 when three agents walk together.

Table 11 shows the average euclidean values and root mean square error values for the test samples. The average values indicate good results as almost all values are less than one, with MED = 0.38 and FDE = 0.16. An RMSE value of zero would tell that the predicted and actual data are almost identical. The closer the RMSE values and euclidean distance are to zero, the better the model performance. The lower values of lateral and longitudinal separation ($d_{i,j}^{\perp}$ and $d_{i,j}^{\parallel}$) between two agents demonstrate the capability of the model-generated trajectories to emulate the actual trajectories, even when subjects are walking in groups.

Table 10 shows the walking gait variations in instances of Case Study 2. In general, the step length remains in the 0.6 to 0.75-meter range, the default step length range in group behavior. The measured gait parameters reflect the underlying strategies that govern the behavioral rules. The variation in gait parameters shows how an individual maintains their step length and step frequency to maintain a group walking behavior. In Table 10, we can see that Agent 2 and Agent 3's step length are almost the same and less than Agent 1, and Agent 2 and Agent 3 have more step frequency, ultimately all three agents in a group maintain similar speed. The results prove humans' innate ability to adapt their gait parameters to maintain a group movement.

TABLE 8. Case study 1 sample results.

Trajectory Screenshot	Generated Trajectories
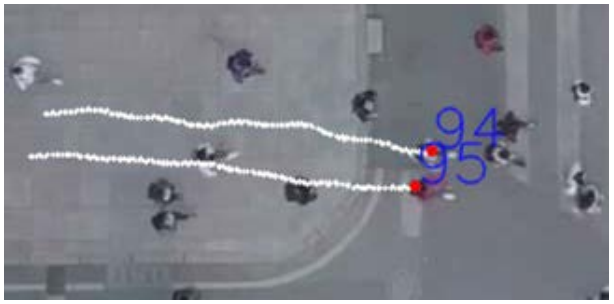 1 (a)	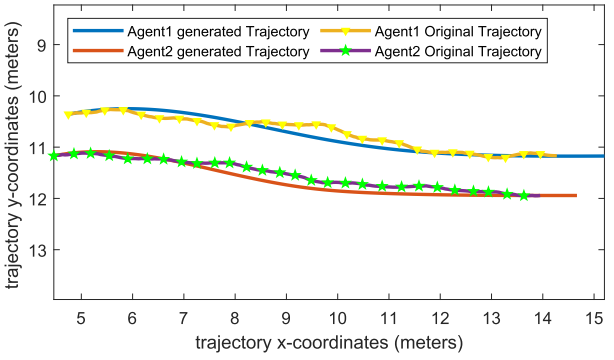 1 (b)
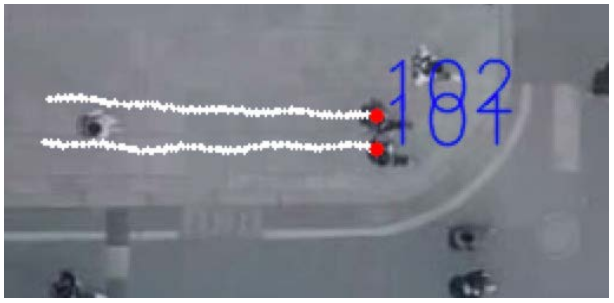 2 (a)	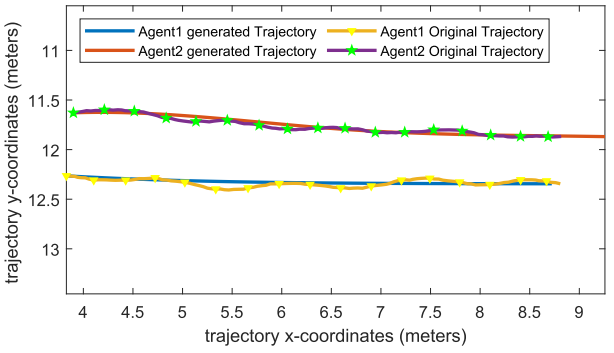 2 (b)
 3 (a)	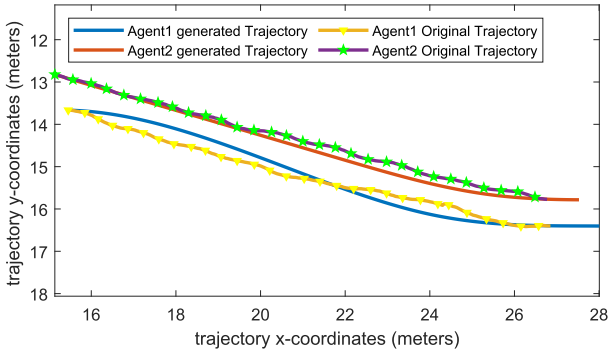 3 (b)

TABLE 9. Table shows detailed performance metric values of case study 1. The average value of the root mean Square Error (rmse) is between the agents' generated coordinates and ground truth coordinates.

Agents' Pair (I and J)	Agent I position		Agent J position		Agent I velocity (rmse_$\vec{v}_i$)	Agent J velocity (rmse_$\vec{v}_j$)	Lateral separation (rmse_$d_{i,j}^{\perp}$)	Longitudinal separation (rmse_$d_{i,j}^{\parallel}$)
	X position (rmse_x1)	Y position (rmse_y1)	X position (rmse_x2)	Y position (rmse_y2)				
94 and 95	0.51	0.15	0.45	0.15	0.43	0.45	0.12	0.005
101 and 102	0.07	0.03	0.22	0.02	0.25	0.41	0.52	0.004
22 and 23	0.9	0.61	0.84	0.67	0.41	0.44	0.21	2.88E-05
53 and 54	0.28	0.4	0.47	0.84	0.26	0.33	0.57	3.55E-05
56 and 57	0.39	0.59	0.37	0.67	0.29	0.31	0.09	6.33E-04
2 and 3	0.09	0.09	0.13	0.4	0.34	0.32	0.04	0.015
7 and 8	0.39	0.29	0.18	0.37	0.46	0.33	0.83	0.0065
16 and 17	0.45	0.15	0.06	0.12	0.36	0.3	0.8	0.003
18 and 19	0.07	0.19	0.43	0.12	0.26	0.4	0.6	0.05
30 and 31	0.6	0.3	0.62	0.2	0.32	0.3	0.06	9.41E-06
32 and 33	0.53	0.33	0.43	0.39	0.33	0.31	0.08	7.66E-06

TABLE 10. (a) Step length (b) Step frequency of agents 101 and 102.

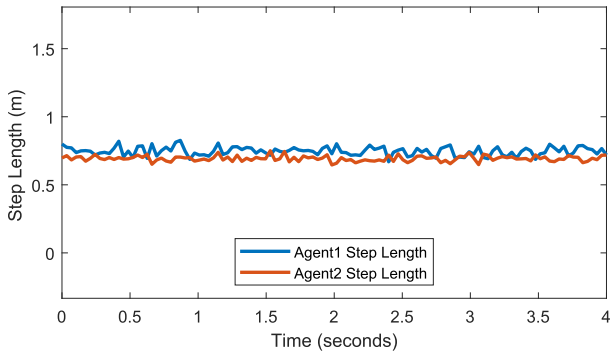

(a)

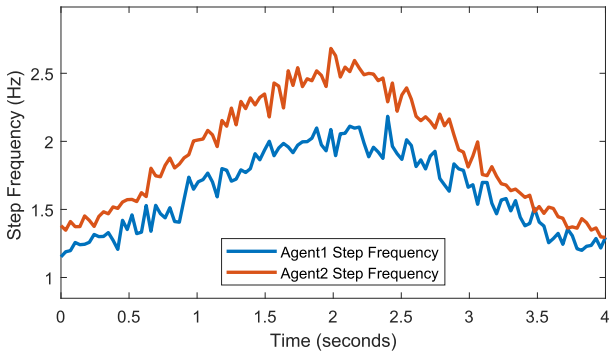

(b)

TABLE 11. Case study 2 performance metrics average values for DUT dataset.

Performance metrics	Average values
MED	0.38
FDE	0.16
rmse_$d^{\perp}_{1,2}$	0.87
rmse_$d^{\parallel}_{1,2}$	0.005
rmse_$d^{\perp}_{2,3}$	0.32
rmse_$d^{\parallel}_{2,3}$	0.002

C. CASE STUDY 3: AN AGENT AVOIDS AN OBSTACLE

1) DESCRIPTION

The third study demonstrates how individuals avoid stationery obstacles. We study the scenarios where the pedestrian passes the stationery obstacle (in our case, it is a standing car represented as a square obstacle). The average buffer zone that pedestrians keep having a safe pass by the obstacle is calculated using data. The estimated buffer zone is approx 0.55 meters. The model is calibrated, and parameters values are listed in Table 6. Twenty case study 3 samples are collected from the dataset, divided the fifteen samples for training the model and five samples for testing the developed model. In the Table 15, the left column has the sample screenshots from actual video data. The right column has the corresponding model-generated pedestrian trajectories.

2) RESULT

Once the model was calibrated, we validated the testing data. The results are shown in Table 15. The table shows the graph which is comparing the actual and predicted trajectories.

The Table 14 shows the average Euclidean distance values. The closer the euclidean distance values are to zero, the better fit the data has achieved. The average values indicate good results as almost all values are under one, with MED = 0.66 and FDE = 0.35.

Table 16 illustrates the obtained gait parameters in Case study 3. The proposed algorithm plans the trajectories based on RHC, which generates the trajectories for a series of short-horizon using the current state values for every horizon calculation. Therefore, while avoiding the stationery obstacle, the algorithm considers the buffer zone around the obstacle and generates a trajectory where the agent maintains the walking speed while adjusting the gait parameters. The step length and step frequency results validate that the agent tries to maintain a constant walking speed by adjusting the gait parameters.

D. CROSS-VALIDATION WITH TrajNet++

TrajNet++ is an interaction-centric trajectory dataset [31]. The data is sampled based on various interaction scenarios. There are leader-follower interactions, group interactions and obstacle avoidance interactions. The TrajNet++ is a current benchmark, and many trajectory forecasting models are using it to validate their efficacy. We have used TrajNet++ to cross-validate our trajectory planning algorithm. The idea is to validate the robustness of the developed algorithm; such the algorithm can be successfully applied to urban traffic scenarios in LA as well as in NYC urban shared space traffic scenarios just by providing the agent's initial and final destination coordinates.

A group interaction scenario of two agents walking together is Case study 1. The calibrated values are provided in the Table 4. We extracted twenty sample trajectories to perform the cross-validation and calculate the performance metrics. Table 17 illustrates the result of two agents walking together. The trajectories with markers are the actual trajectories of two pedestrians, and the non-marker trajectories are model-generated trajectories. The calculated performance metrics are shown below in Table 18. The evaluation metrics in the table have values less than one, which demonstrates the good performance of the approach.

A group interaction scenario of three agents walking together is Case study 2. The calibrated values are provided in Table 5. We extracted fifteen sample trajectories to perform the cross-validation and calculate the performance metrics. The calculated performance metrics are shown in

TABLE 12. Case study 2 sample results.

Trajectory Screenshot	Generated Trajectories
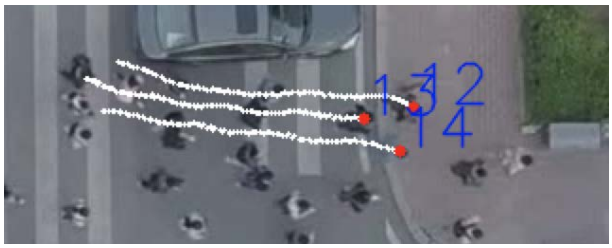	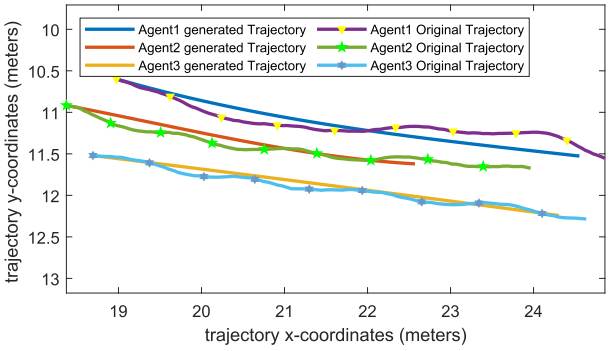
1 (a)	1 (b)
	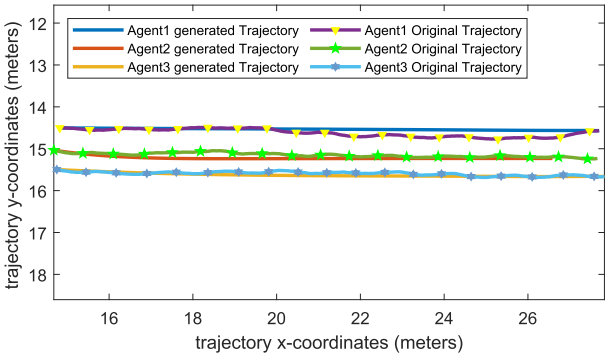
2 (a)	2 (b)

TABLE 13. (a) Step length (b) Step frequency of agents 22, 23, and 24.

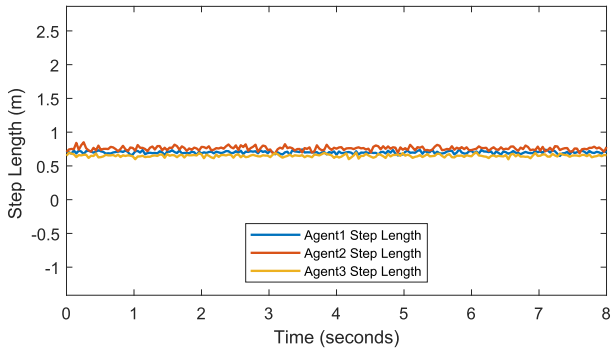

(a)

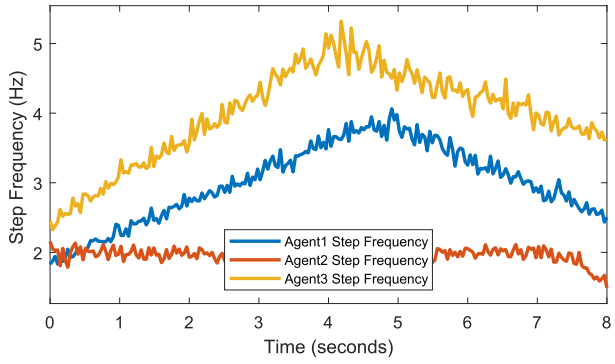

(b)

TABLE 14. Case study 3 performance metrics average values for DUT dataset.

Performance metrics	Average values
MED	0.66
FDE	0.35

Table 19. Almost all error metrics values are less than one, except root mean square error in the lateral separation value between two agents, which is close to one. The pedestrian group interaction is very complex and involves multiple behavioral factors. There are in-group interactions and group-surrounding interactions that affect the trajectories; which justifies the observed results. The algorithm performance for Case study 3, where the pedestrian passes the stationery obstacle (in our case, a standing car represented as a square), is also cross-validated. Refer the Table 6 for model calibrated values. We extracted ten sample trajectories to perform the cross-validation and calculate the performance metrics. The performance metrics are shown in Table 20. The MED = 0.78 and FDE = 0.45, again reassures the algorithms' performance.

TABLE 15. Case study 3: sample results.

Trajectory Screenshot	Generated Trajectories
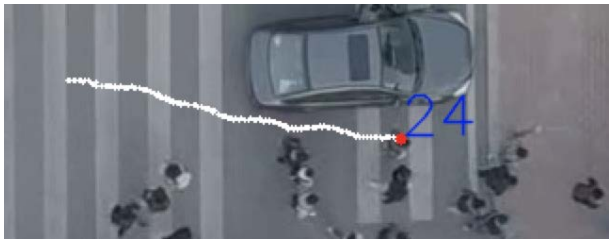 1 (a)	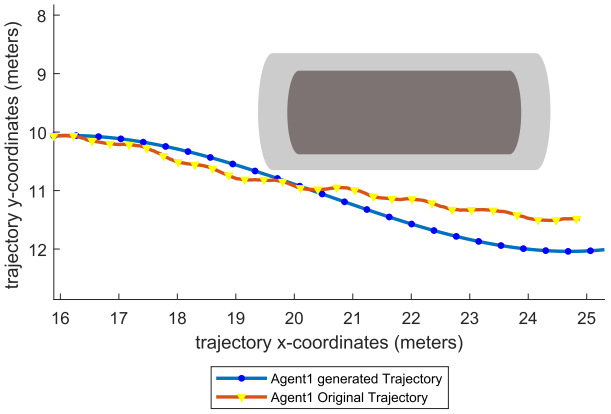 1 (b)
 2 (a)	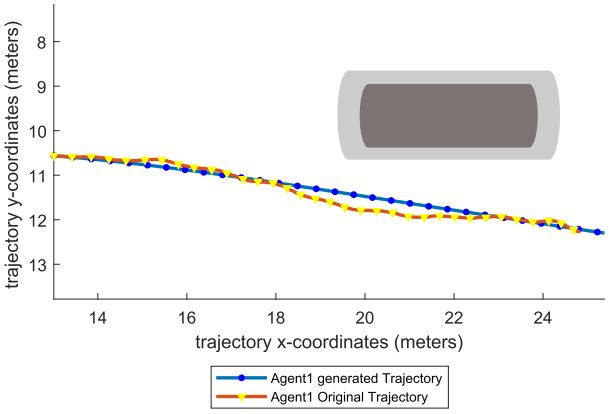 2 (b)

TABLE 16. (a) Step length (b) Step frequency of an agent avoiding an obstacle.

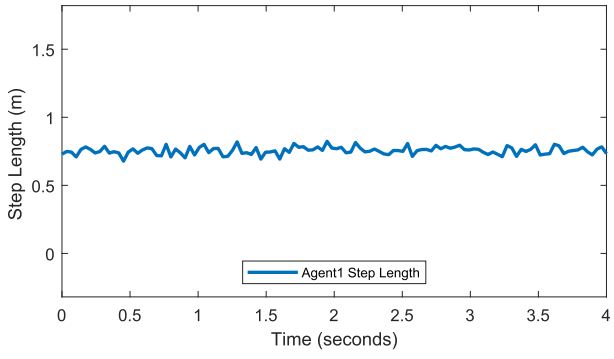

(a)

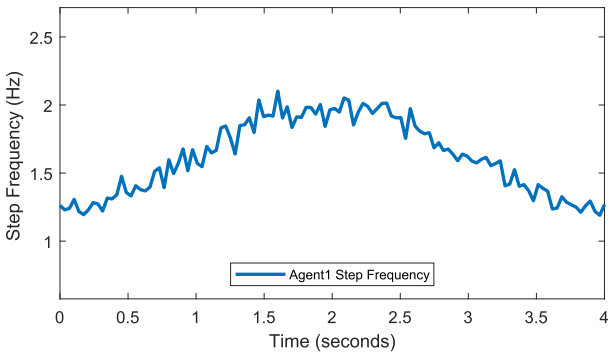

(b)

E. BASELINE COMPARISON

In this section, we provide a comparative summary of the performance of our approach with existing machine learning algorithms for trajectory generation. However, it is important to note that a direct comprehensive comparison is not possible given the "black box" nature of the algorithms. Also, the role of the machine learning models is different from the generative approach adopted in our paper. Mostly, machine learning models are prediction models. It means that a model predicts the pedestrians' spatial coordinates in the near future (let's say for 4-5 seconds) using some historical observations. The predictive models are also trained on large datasets.

TABLE 17. Cross validation with TrajNet++ (showing trajectory generation for case study 1: Two agents walking together).

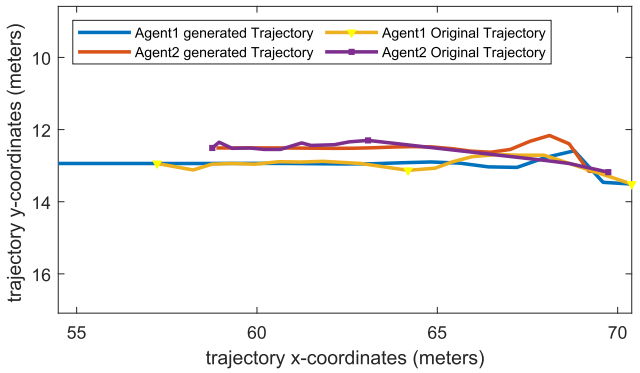

TABLE 18. Case study 1 performance metrics average values in TrajNet++ dataset.

Performance metrics	Average values
MED	0.32
FDE	0.41
rmse_$d^{\perp}_{i,j}$	0.40
rmse_$d^{\parallel}_{i,j}$	0.01

TABLE 19. Case study 2 performance metrics average values in TrajNet++ dataset.

Performance metrics	Average values
MED	0.39
FDE	0.18
rmse_$d^{\perp}_{1,2}$	1.05
rmse_$d^{\parallel}_{1,2}$	0.01
rmse_$d^{\perp}_{2,3}$	0.9
rmse_$d^{\parallel}_{2,3}$	0.04

TABLE 20. Case study 3 performance metrics average values in TrajNet++ dataset.

Performance metrics	Average values
MED	0.78
FDE	0.45

The training prepares the model to capture the underlying social norms and generalize the models for the various scenarios. However, this is very challenging as the training data often only contains examples from safe surroundings with very few occurrences of dangerous scenarios. On the other hand, our generative approach is fully defined, parameterized and can be tuned as needed. It does not require prior training and once the model parameters are calibrated, the model is fit to generate trajectories for various scenarios. Table 21 compares the MED and FED for state of the art models and for our algorithm in the three case studies using the TrajNet++ dataset. Note that the proposed approach has comparable (or even better) error metrics. However, the comparison table should be interpreted subjectively since, as we stated earlier, the model objectives are not aligned.

TABLE 21. Performance metrics comparison chart for different pedestrian trajectory forecasting models based on TrajNet++ dataset .

Experimental Results for TrajNet++ dataset	Performance Metrics	
	MED	FDE
PecNet [65][66]	0.57	1.18
AIN [67] [66]	0.62	1.24
Social NCE [68] [66]	0.53	1.14
AMENet [69] [66]	0.62	1.30
Proposed Approach - Case Study1	0.32	0.41
Proposed Approach - Case Study2	0.39	0.18
Proposed Approach - Case Study3	0.78	0.45

VI. CONCLUSION AND FUTURE WORK

This paper proposed a novel methodology to generate pedestrian trajectories while interacting with other pedestrians and stationary obstacles (infrastructure obstacles or other types of road users). The model can generate pedestrian trajectories for traffic scenarios based on the road users' behavior and interaction rules. The methodology utilized mixed-integer linear programming embedded in the receding horizon control framework for trajectory generation. Validation was performed on two publicly available real datasets. The evaluation metrics, mean euclidean distance, and final displacement error yielded near-zero values, demonstrating the promising performance of the proposed generative trajectory planning model. The obtained gait parameters are also consistent with the previous studies on how pedestrians adjust their gait in different scenarios. Cross-validation with TrajNet++ was also performed to validate the algorithm's robustness.

The proposed approach is flexible to adapt to the need of various traffic scenarios. The generative pedestrian trajectory model can simulate a broad range of pedestrian traffic scenarios. A case-specific pedestrian behavior can be directly incorporated into the cost function or constraints to customize the proposed model further. One can perform parameter tuning to test the behavior and trajectory generation in various traffic scenarios. One can also input the commonality attribute to permit the distinction of a pedestrian group. The proposed algorithm lies between the two sets of modeling paradigms — the black-box algorithms (such as machine learning), which are hard to interpret and parameterize, and the analytical modeling with a set of parametrized equations. In summary, the proposed model is fully defined and parametrized with pedestrians' behavioral rules, and gait parameters can serve as a basis for exploring pedestrian behavior in different scenarios. The benefit of the receding-horizon control framework is the capability of modeling traffic uncertainties and pedestrian response to the uncertainties.

The developed pedestrian trajectory planning model, expanded as a simulation framework, will provide a more realistic demonstration of how pedestrians use traffic facilities and interact with their environment. The traffic simulation tool results will help propose traffic rules to optimize the traffic flows and infrastructure and plan ideas suitable

for shared spaces. Moreover, the model's applicability is not limited to road traffic and shared spaces. It can find broader applications such as the emergency evacuation of buildings, large events, airports, and railway stations. Note that the developed model also supports encounter modeling which is essential in air traffic control to develop and test collision avoidance systems [70]. This paper focused on the pedestrians' primary behavior and social interaction scenarios. In future work, we will expand the research to include the more complex social interaction traffic scenarios and varying degrees of density. The developed model will be extended to consider pedestrian behavioral and social interaction rules while interacting with moving obstacles and varying uncertainties in the traffic environment. We will also model the pedestrian dynamics by considering attributes like age, gender, and distractions that impact the walking gait characteristics. We will also expand the work to model other VRUs like cyclists and scooter users.

REFERENCES

[1] U. Desa, *68% of the World Population Projected to Live in Urban Areas by 2050*, United Nations Department of Economic and Social Affairs, New York, NY, USA, 2018.
[2] A. Gill, "Changing cities and minds for active mobility," Scholar-Bank@NUS Repository, Nat. Univ. Singapore, Singapore, Apr. 2018, pp. 1–24, doi: 10.25818/qfk4-d7za.
[3] *Safety of Vulnerable Road Users*, Directorate for Science, Technology and Industry, Programme of Cooperation in the Field of Research on Road Transport and Intermodal Linkages, Washington, DC, USA, 1998. Accessed: Nov. 30, 2021.
[4] *Comparing Demographic Trends in Vulnerable Road User Fatalities and the U.S. Population, 1980–2019*, NHTSA Traffic Safety Facts Research Note, Washington, DC, USA, 2021. Accessed: Dec. 2, 2021.
[5] *Overview of Motor Vehicle Crashes in 2019*, NHTSA Traffic Safety Facts Research Note, Washington, DC, USA, 2020. Accessed: Jan. 26, 2022.
[6] B. Hamilton-Baillie, "Shared space: Reconciling people, places and traffic," *Built Environ.*, vol. 34, no. 2, pp. 161–181, May 2008.
[7] E. Jaffe, "6 places where cars, bikes, and pedestrians all share the road as equals," Bloomberg CityLab, Washington, DC, USA, Tech. Rep. 2015, 2021. Accessed: Dec. 3, 2021.
[8] B. C. Tefft, L. S. Arnold, and W. J. Horrey, "Examining the increase in pedestrian fatalities in the United States, 2009–2018 (research brief)," AAA Found. Traffic Saf., Washington, DC, USA, 2021.
[9] *Pedestrian Traffic Fatalities by State: 2019 Preliminary Data*, GHSA Annual Spotlight Report, Washington, DC, USA, 2020. Accessed: Nov. 22, 2021.
[10] S. P. Hoogendoorn and P. H. Bovy, "Normative pedestrian behaviour theory and modelling," in *Transportation and Traffic Theory in the 21st Century*. Bingley: U.K.: Emerald Group Publishing Ltd., 2002.
[11] Y. Guo, G. Xu, and S. Tsuji, "Understanding human motion patterns," in *Proc. 12th IAPR Int. Conf. Pattern Recognit.*, vol. 2, Oct. 1994, pp. 325–329.
[12] S. Hoogendoorn and P. H. L. Bovy, "Gas-kinetic modeling and simulation of pedestrian flows," *Transp. Res. Rec.*, vol. 1710, no. 1, pp. 28–36, Jan. 2000.
[13] V. J. Blue and J. L. Adler, "Cellular automata microsimulation for modeling bi-directional pedestrian walkways," *Transp. Res. B, Methodol.*, vol. 35, no. 3, pp. 293–312, Mar. 2001.
[14] J. K. Aggarwal and Q. Cai, "Human motion analysis: A review," *Comput. Vis. Image Understand.*, vol. 73, no. 3, pp. 428–440, Mar. 1999.
[15] L. Wang, W. Hu, and T. Tan, "Recent developments in human motion analysis," *Pattern Recognit.*, vol. 36, no. 3, pp. 585–601, 2003.
[16] D. Metaxas and S. Zhang, "A review of motion analysis methods for human nonverbal communication computing," *Image Vis. Comput.*, vol. 31, nos. 6–7, pp. 421–433, Jun. 2013.
[17] H. Barbosa, M. Barthelemy, G. Ghoshal, C. R. James, M. Lenormand, T. Louail, R. Menezes, J. J. Ramasco, F. Simini, and M. Tomasini, "Human mobility: Models and applications," *Phys. Rep.*, vol. 734, pp. 1–74, Mar. 2018.
[18] T. B. Moeslund, A. Hilton, and V. Krüger, "A survey of advances in vision-based human motion capture and analysis," *Comput. Vis. Image Understand.*, vol. 104, nos. 2–3, pp. 90–126, 2006.
[19] C. Gloor, P. Stucki, and K. Nagel, "Hybrid techniques for pedestrian simulations," in *Proc. Int. Conf. Cellular Automata*. Berlin, Germany: Springer, 2004, pp. 581–590.
[20] T. Kretz, "Pedestrian traffic: Simulation and experiments," Ph.D. dissertation, Dept. Phys., Duisburg, Essen, Univ., Duisburg, Germany, 2007.
[21] T. Robin, G. Antonini, M. Bierlaire, and J. Cruz, "Specification, estimation and validation of a pedestrian walking behavior model," *Transp. Res. B, Methodol.*, vol. 43, no. 1, pp. 36–56, 2009.
[22] M. Chraibi, U. Kemloh, A. Schadschneider, and A. Seyfried, "Force-based models of pedestrian dynamics," *Netw. Heterogeneous Media*, vol. 6, no. 3, p. 425, 2011.
[23] G. Waizman, S. Shoval, and I. Benenson, "Micro-simulation model for assessing the risk of vehicle–pedestrian road accidents," *J. Intell. Transp. Syst.*, vol. 19, no. 1, pp. 63–77, Jan. 2015.
[24] L. Crociani, G. Vizzari, D. Yanagisawa, K. Nishinari, and S. Bandini, "Route choice in pedestrian simulation: Design and evaluation of a model based on empirical observations," *Intelligenza Artif.*, vol. 10, no. 2, pp. 163–182, Jan. 2016.
[25] D. Helbing, *Social Self-Organization: Agent-Based Simulations and Experiments to Study Emergent Social Behavior*. Berlin, Germany: Springer, 2012.
[26] M. Seitz, G. Köster, and A. Pfaffinger, "Pedestrian group behavior in a cellular automaton," in *Pedestrian and Evacuation Dynamics*. Cham, Switzerland: Springer, 2014, pp. 807–814.
[27] A. Schadschneider, "Cellular automaton approach to pedestrian dynamics-theory," 2001, *arXiv:cond-mat/0112117*.
[28] H. Kuehne, H. Jhuang, E. Garrote, T. Poggio, and T. Serre, "HMDB: A large video database for human motion recognition," in *Proc. Int. Conf. Comput. Vis.*, Nov. 2011, pp. 2556–2563.
[29] A. Rudenko, L. Palmieri, M. Herman, K. M. Kitani, D. M. Gavrila, and K. O. Arras, "Human motion trajectory prediction: A survey," *Int. J. Robot. Res.*, vol. 39, no. 8, pp. 895–935, 2020.
[30] D. Yang, L. Li, K. Redmill, and U. Ozguner, "Top-view trajectories: A pedestrian dataset of vehicle-crowd interaction from controlled experiments and crowded campus," in *Proc. IEEE Intell. Vehicles Symp. (IV)*, Jun. 2019, pp. 899–904.
[31] P. Kothari, S. Kreiss, and A. Alahi, "Human trajectory forecasting in crowds: A deep learning perspective," *IEEE Trans. Intell. Transp. Syst.*, vol. 23, no. 7, pp. 7386–7400, Jul. 2022.
[32] C. G. Keller and D. M. Gavrila, "Will the pedestrian cross? A study on pedestrian path prediction," *IEEE Trans. Intell. Transp. Syst.*, vol. 15, no. 2, pp. 494–506, Apr. 2014.
[33] T. Gandhi and M. M. Trivedi, "Pedestrian protection systems: Issues, survey, and challenges," *IEEE Trans. Intell. Transp. Syst.*, vol. 8, no. 3, pp. 413–430, Sep. 2007.
[34] S. P. Hoogendoorn, "Microscopic pedestrian wayfinding and dynamics modeling," in *Pedestrian and Evacuation Dynamics*. Berlin, Germany: Springer, 2001.
[35] D. Helbing and P. Molnár, "Social force model for pedestrian dynamics," *Phys. Rev. E, Stat. Phys. Plasmas Fluids Relat. Interdiscip. Top.*, vol. 51, no. 5, p. 4282, 1995.
[36] V. J. Blue and J. L. Adler, "Emergent fundamental pedestrian flows from cellular automata microsimulation," *Transp. Res. Rec., J. Transp. Res. Board*, vol. 1644, no. 1, pp. 29–36, 1998.
[37] J. Dijkstra, A. J. Jessurun, and H. J. P. Timmermans, "A multi-agent cellular automata model of pedestrian movement," in *Pedestrian and Evacuation Dynamics*, M. Schreckenberg and S. D. Sharma, Eds. Berlin, Germany: Springer-Verlag, 2001, pp. 173–181.
[38] S. P. Hoogendoorn and P. H. Bovy, "Pedestrian route-choice and activity scheduling theory and models," *Transp. Res. B, Methodol.*, vol. 38, no. 2, pp. 169–190, 2004.
[39] E. Keogh, T. Palpanas, V. B. Zordan, D. Gunopulos, and M. Cardle, "Indexing large human-motion databases," in *Proc. 30th Int. Conf. Very Large Data Bases*, vol. 30, 2004, pp. 780–791.
[40] R. Blake and M. Shiffrar, "Perception of human motion," *Annu. Rev. Psychol.*, vol. 58, pp. 47–73, Jan. 2007.
[41] R. Poppe, "Vision-based human motion analysis: An overview," *Comput. Vis. Image Understand.*, vol. 108, nos. 1–2, pp. 4–18, Oct. 2007.

[42] S. Zhou, D. Chen, W. Cai, L. Luo, M. Y. H. Low, F. Tian, V. S.-H. Tay, D. W. S. Ong, and B. D. Hamilton, "Crowd modeling and simulation technologies," *ACM Trans. Model. Comput. Simul.*, vol. 20, no. 4, pp. 1–35, Nov. 2010, doi: 10.1145/1842722.1842725.

[43] D. C. Duives, W. Daamen, and S. P. Hoogendoorn, "State-of-the-art crowd motion simulation models," *Transp. Res. C, Emerg. Technol.*, vol. 37, pp. 193–209, Dec. 2013.

[44] N. Jennings, "On agent-based software engineering," *Artif. Intell.*, vol. 117, pp. 277–296, Dec. 2002.

[45] P. Wegner, "Why interaction is more powerful than algorithms," *Commun. ACM*, vol. 40, no. 5, pp. 80–91, May 1997.

[46] T. Schelhorn, D. O'Sullivan, M. Haklay, and M. Thurstain-Goodwin, "STREETS: An agent-based pedestrian model," Centre Adv. Spatial Anal., FrancoAngeli, Milan, Italy, CASA Working Paper 9, 1999.

[47] M. H. Zaki and T. Sayed, "Automated analysis of pedestrian group behavior in urban settings," *IEEE Trans. Intell. Transp. Syst.*, vol. 19, no. 6, pp. 1880–1889, Jun. 2018.

[48] M. H. Zaki and T. Sayed, "Automated classification of road-user movement trajectories," *Transp. Res. C*, vol. 33, pp. 50–73, Jan. 2013.

[49] H. Hediyeh, T. Sayed, M. H. Zaki, and G. Mori, "Pedestrian gait analysis using automated computer vision techniques," *Transportmetrica A, Transp. Sci.*, vol. 10, no. 3, pp. 214–232, Mar. 2014.

[50] A. Getchell, "Agent-based modeling," *Physics*, vol. 22, no. 6, pp. 757–767, 2008.

[51] M. Hussein, "Development of an agent based simulation model for pedestrian interactions," Ph.D. dissertation, Dept. Civil Eng., Univ. Brit. Columbia, Vancouver, BC, Canada, 2016.

[52] D. Ridel, E. Rehder, M. Lauer, C. Stiller, and D. Wolf, "A literature review on the prediction of pedestrian behavior in urban scenarios," in *Proc. 21st Int. Conf. Intell. Transp. Syst. (ITSC)*, Nov. 2018, pp. 3105–3112.

[53] J. Li, F. Yang, M. Tomizuka, and C. Choi, "EvolveGraph: Multi-agent trajectory prediction with dynamic relational reasoning," 2020, *arXiv:2003.13924*.

[54] H. Zhao, J. Gao, T. Lan, C. Sun, B. Sapp, B. Varadarajan, Y. Shen, Y. Shen, Y. Chai, C. Schmid, C. Li, and D. Anguelov, "TNT: Target-driveN trajectory prediction," 2020, *arXiv:2008.08294*.

[55] H. Xue, D. Q. Huynh, and M. Reynolds, "SS-LSTM: A hierarchical LSTM model for pedestrian trajectory prediction," in *Proc. IEEE Winter Conf. Appl. Comput. Vis. (WACV)*, Mar. 2018, pp. 1186–1194.

[56] P. Zhang, W. Ouyang, P. Zhang, J. Xue, and N. Zheng, "SR-LSTM: State refinement for LSTM towards pedestrian trajectory prediction," in *Proc. IEEE/CVF Conf. Comput. Vis. Pattern Recognit. (CVPR)*, Jun. 2019, pp. 12085–12094.

[57] M. Moussaïd, N. Perozo, S. Garnier, D. Helbing, and G. Theraulaz, "The walking behaviour of pedestrian social groups and its impact on crowd dynamics," *PLoS ONE*, vol. 5, no. 4, Apr. 2010, Art. no. e10047.

[58] W. Ge, R. T. Collins, and R. B. Ruback, "Vision-based analysis of small groups in pedestrian crowds," *IEEE Trans. Pattern Anal. Mach. Intell.*, vol. 34, no. 5, pp. 1003–1016, May 2012.

[59] W. Daamen and S. P. Hoogendoorn, "Experimental research of pedestrian walking behavior," *Transp. Res. Rec.*, vol. 1828, no. 1, pp. 20–30, Jan. 2003.

[60] J. Drury, C. Cocking, and S. Reicher, "Everyone for themselves? A comparative study of crowd solidarity among emergency survivors," *Brit. J. Social Psychol.*, vol. 48, no. 3, pp. 487–506, Sep. 2009.

[61] C. Wan, L. Wang, and V. V. Phoha, "A survey on gait recognition," *ACM Comput. Surv.*, vol. 51, no. 5, pp. 1–35, 2018.

[62] T. Öberg, A. Karsznia, and K. Öberg, "Basic gait parameters: Reference data for normal subjects, 10–79 years of age," *J. Rehabil. Res. Develop.*, vol. 30, p. 210, Jan. 1993.

[63] R. B. Dale, "21—Clinical gait assessment," in *Physical Rehabilitation of the Injured Athlete*, J. R. Andrews, G. L. Harrelson, and K. E. Wilk, Eds., 4th ed. Philadelphia, PA, USA: Saunders, 2012, pp. 464–479. [Online]. Available: https://www.sciencedirect.com/science/article/pii/B9781437724110000216

[64] M. Matte, "Does stride length affect the speed you walk?" Chron, Houston, TX, USA, Tech. Rep., 2018. Accessed: Apr. 26, 2022.

[65] K. Mangalam, H. Girase, S. Agarwal, K.-H. Lee, E. Adeli, J. Malik, and A. Gaidon, "It is not the journey but the destination: Endpoint conditioned trajectory prediction," in *Proc. Eur. Conf. Comput. Vis.* Cham, Switzerland: Springer, 2020, pp. 759–776.

[66] R. Rozenberg, J. Gesnouin, and F. Moutarde, "Asymmetrical bi-RNN for pedestrian trajectory encoding," 2021, *arXiv:2106.04419*.

[67] Y. Zhu, D. Ren, M. Fan, D. Qian, X. Li, and H. Xia, "Robust trajectory forecasting for multiple intelligent agents in dynamic scene," 2020, *arXiv:2005.13133*.

[68] Y. Liu, Q. Yan, and A. Alahi, "Social NCE: Contrastive learning of socially-aware motion representations," in *Proc. IEEE/CVF Int. Conf. Comput. Vis. (ICCV)*, Oct. 2021, pp. 15118–15129.

[69] H. Cheng, W. Liao, M. Y. Yang, B. Rosenhahn, and M. Sester, "AMENet: Attentive maps encoder network for trajectory prediction," *ISPRS J. Photogramm. Remote Sens.*, vol. 172, pp. 253–266, Feb. 2021.

[70] A. Weinert, S. Campbell, A. Vela, D. Schuldt, and J. Kurucar, "Well-clear recommendation for small unmanned aircraft systems based on unmitigated collision risk," *J. Air Transp.*, vol. 26, no. 3, pp. 113–122, Jul. 2018.

SAUMYA GUPTA (Student Member, IEEE) received the B.S. degree in electronics and instrumentation engineering from Uttar Pradesh Technical University, India, and the M.S. degree in electrical engineering from the University of Nevada Las Vegas (UNLV), Las Vegas, NV, USA. She is currently pursuing the Ph.D. degree in civil engineering with the University of Central Florida (UCF), Orlando, Florida. From 2014 to 2016, she was a Research Assistant with the Transportation Research Center, UNLV. From 2016 to 2018, she worked as a Data Scientist at PolyPak America, Los Angeles, California. She was also an Adjunct Professor in electrical engineering at California State University Los Angeles (CSULA), from 2017 to 2018. Since 2018, she has been a Ph.D. Student and a Research Assistant with the DTES Laboratory, UCF. Over the period, she has evolved her background in control theories and their application in transportation systems. She authored one IEEE journal article and several other conference papers. Her research interests include optimization, modeling and simulation, active mobility, pedestrian behavior and interactions, urban planning, and sustainability.

MOHAMED H. ZAKI (Member, IEEE) received the Ph.D. degree from the Hardware Verification Group, Concordia University, Montreal, in 2008. He is currently an Assistant Professor in transportation engineering with the Civil, Environmental & Construction Engineering Department, University of Central Florida. Before, he was a Research Associate with the Bureau of Intelligent Transportation Systems and Freight Security, The University of British Columbia. His multidisciplinary research focuses on solving tomorrow's smart cities problems; from the computing and information to its facilities infrastructure. He studies road safety and road-user's behavior through the automated analysis of traffic data. He serves on the Transportation Research Board (TRB) AED50 Committee on Artificial Intelligence and Advanced Computing Applications.

ADAN VELA received the Ph.D. degree in mechanical engineering from the Georgia Institute of Technology. He currently holds the rank of an Assistant Professor with the Industrial Engineering and Management Systems Department, University of Central Florida. Prior to his academic post, he served as a member of the Technical Staff with the MIT Lincoln Laboratory. Over the past 20 years, he has developed an Expertise in the modeling, simulation, and optimization of complex traffic systems, with focused research interest in those systems that involve human-in-the-loop control and intelligent decision systems.